

1 **A rheological characterization of mashed potatoes enriched with soy**  
2 **protein isolate**

3  
4 María Dolores Alvarez<sup>\*</sup>, Cristina Fernández, María Dolores Olivares,  
5 Wenceslao Canet  
6

7  
8 *Department of Characterization, Quality and Food Safety, **Institute of Food Science, Technology and Nutrition***  
9 *(**ICTAN-CSIC**), José Antonio Novais 10, Ciudad Universitaria, E-28040 Madrid, Spain*  
10

11  
12 *Abbreviated running title*

13 Rheology of soy protein isolate-enriched mashed potatoes  
14  
15  
16  
17  
18  
19  
20  
21  
22  
23  
24  
25  
26  
27

28 <sup>\*</sup>Corresponding author. Tel.: +34 915492300; fax +34 915493627.  
29 *E-mail address:* [mayoyes@ictan.csic.es](mailto:mayoyes@ictan.csic.es) (M.D. Alvarez).  
30

31 ABSTRACT

32

33 The effect of the addition of soy protein isolate (SPI) (0, 15, 30, 45 and 60 g kg<sup>-1</sup>) on  
34 viscoelastic properties, large deformation measurements and microstructure of fresh (FM) and  
35 frozen/thawed (F/TM) mashed potatoes was investigated. Rheological data showed weak gel  
36 behaviour for both FM and F/TM potatoes without and with added SPI together with a  
37 significant decrease of system viscoelasticity ( $G'$  and  $G''$ ) with increasing SPI volume  
38 fraction, primarily attributed to the no interaction between the amylose/amylopectine matrix  
39 and the dispersed SPI particles or aggregates as revealed by scanning electron microscopy  
40 (SEM). Micrographs also showed that SPI formed white coarse aggregates. A freeze/thaw  
41 cycle produced a more significant decrease in viscoelastic functions, due to superior  
42 aggregation of denatured SPI and reduced water activity. In F/TM samples, high correlations  
43 between small and large deformation measurements were found. Results may be useful for  
44 technological applications in SPI-enriched mashed potatoes.

45

46 *Keywords:*

47 Soy protein isolate

48 Hydrocolloids

49 Freezing

50 Mechanical spectra

51 Phase separation

52 Texture

53

54 **1. Introduction**

55

56 In recent years, considerable interest has been given to the study of protein-polysaccharide  
57 mixtures in both the industrial and academic sectors (Zhu, Yang, Ahmad, Li, Wang, & Liu,  
58 2008). Protein and starch are present in many foods and they contribute to their structural and  
59 textural characteristics through their aggregation and gelation behaviour. The overall texture  
60 and stability of food products depend not only on the properties of proteins and  
61 polysaccharides, but also on the nature and strength of protein/polysaccharide interaction  
62 (Hemar, Hall, Munro, & Singh, 2002). Therefore, a knowledge of the mechanisms of  
63 interactions occurring in protein-polysaccharide systems is important in developing desirable  
64 properties in food products. In addition, great potential remains in mixing polysaccharides  
65 with globular proteins, soy protein isolate.

66 Potato starches are attractive food ingredients because they are both natural and safe,  
67 whereas soy proteins are typical vegetable proteins with health-enhancing activities. Soy-  
68 based food consumption has been on the rise since the US Food and Drug Administration  
69 (FDA) decided to accept soy protein health claims linking the intake of products high in soy  
70 protein with several potential health benefits. Functional properties of soybean protein isolates  
71 (SPI) reflect the composition, structure, denaturation, and degree of aggregation of their major  
72 components: 7S ( $\beta$ -conglycinin) and 11S (glycinin) globulins (Puppo, Sorgentini, & Añón,  
73 2000).

74 An important functional property in SPI is gelation during thermal treatment with  
75 desirable water holding capacity. Heat treatment induces dissociation, denaturation and  
76 aggregation of soy protein (Sorgentini, Wagner, & Añón, 1995). Freezing also brought about  
77 some changes in the processing characteristics of soybeans. When the soy protein solution  
78 was frozen, the proteins became partially insoluble due to the polymerization of protein

79 molecules through the formation of intermolecular disulphide bonds ([Hashizume, Kakiuchi,](#)  
80 [Koyama, & Watanabe, 1971](#)). However, only a few studies have been carried out to  
81 characterize the freezing effect on soy protein properties ([Li, Li, Hua, Qiu, Yang, & Cui,](#)  
82 [2007](#)).

83 There is a possibility of using SPIs in combination with potato products, not only to  
84 provide a useful alternative to other highly nutritious and healthy food products, but also to  
85 improve the physicochemical, functional and sensory characteristics of potato products in  
86 general. Research on the influence of food ingredients and food processing conditions on SPI  
87 performance in specific foods is scarce. Mashed potatoes (MP) are a promising nutritious  
88 vehicle for incorporating soy into the diet. Nevertheless, FM potatoes themselves make up a  
89 combined system of native potato starch, denatured milk protein, water and salt plus added  
90 cryoprotectants [xanthan gum (XG) and kappa-carrageenan ( $\kappa$ -C)] as the product is intended  
91 to be frozen. During the MP preparation procedure (heating), starch, XG,  $\kappa$ -C and protein  
92 undergo physicochemical changes, such as starch gelatinization and solubilization, protein  
93 denaturation and hydrogen bond rupture. After heating, when MP samples are cooled to 55  
94 °C, changes in starch, XG and  $\kappa$ -C polymers occur and continuous and dispersed phase  
95 properties are influenced. Consequently, as complex interactions can influence the properties  
96 of these mixtures, structural changes produced in MPs as a result of SPI addition, heating and  
97 freeze/thaw cycle need to be monitored directly in the MP matrix.

98 Many food products are macromolecular gels containing dispersed particles (fillers) ([van](#)  
99 [Vliet, 1988](#)). The influence of these particles on the rheological properties of a gel can be  
100 drastic, depending on their concentration and rheological properties and on the extent of filler-  
101 gel matrix interaction. In MPs with added SPI, the rheological properties will depend on  
102 whether the SPI gel was formed or not, and on gel type, both factors being dependent on the  
103 degree of denaturation and the extent of protein aggregation reached ([Sorgentini et al., 1995](#)).

104 Small amplitude oscillatory shear (SAOS) measurements afford the measurement of  
105 dynamic rheological functions, without altering the internal network structure of materials  
106 tested (Alvarez, Fernández, Solas, & Canet, 2011; Campo-Deaño, Tovar, & Borderías, 2010).  
107 The gelation behaviour and characteristics of SPI-enriched MPs during heating and  
108 freeze/thaw process could be well represented by SAOS measurements where the strain is  
109 restricted to less than 5%. However, since foodstuffs are subjected to large deformations,  
110 priority should be given to analyzing both linear and nonlinear viscoelastic ranges to  
111 determine product performance under actual processing conditions and consumption  
112 (Navarro, Martino, & Zaritzky, 1997).

113 Given the demand for new functional ingredients in the food industry, characterization of  
114 MPs with added SPIs is worthwhile, as it will aid in extending its possible uses and added  
115 value to this protein. The objective of the present work was to evaluate the effect of the SPI  
116 concentration on viscoelastic properties, large deformation measurements and microstructure  
117 of FM and F/TM potatoes and accordingly to highlight the extent upon which SPI can be  
118 employed without negative changes in mashed potatoes texture characteristics.

119

## 120 **2. Materials and methods**

121

### 122 *2.1. Materials*

123

124 The potatoes used were tubers (*Solanum tuberosum*, L., cv Kennebec) from Aguilar de  
125 Campoo (Burgos, Spain). Readily dispersible SPI with the trade name PRO-FAM<sup>®</sup> 646  
126 (ADM, Netherlands) was used in this study without more purification. The proximate  
127 composition (g/100g), as specified by the producer, was as follows: protein ( $N \times 6.25$ )>90,  
128 moisture<6.0, fat<5, and ash<5. XG (Keltrol F [E]) and  $\kappa$ -C (GENULACTA carrageenan type  
129 LP-60) were donated by Premium Ingredients, S.L. (Girona, Spain). The FDA has determined

130 that diets containing 25 g of soy protein (four daily servings of 6.25 g soy protein) can reduce  
131 levels of low-density lipoproteins (bad cholesterol) by as much as 10 percent ([Federal  
132 Register 1998](#)). Range-finding experiments were carried out by adding four different  
133 concentrations of SPI (15, 30, 45 and 60 g kg<sup>-1</sup>) to the MPs, and MPs without added SPI were  
134 also prepared (0 g kg<sup>-1</sup>) for use as controls. Therefore, an MP serving of 200 g with added SPI  
135 concentrations of 15-60 g kg<sup>-1</sup> would provide from 3-12 g of soy protein respectively. Though  
136 the quantity of 25 g soy protein seems high, soy protein is actually easy to consume, and there  
137 are many examples of different foods with high soy protein content ([http://www.soya.be/soy-  
138 protein-health-claim.php](http://www.soya.be/soy-protein-health-claim.php)). In [Table 1](#) each of the FM and F/TM tested samples can be easily  
139 identified by the notations used.

140

## 141 *2.2 Preparation of MP samples*

142

143 Tubers were manually washed, peeled and diced. MPs were prepared in ~ 1350-g batches  
144 from 607.7 g kg<sup>-1</sup> of potatoes, 230.8 g kg<sup>-1</sup> of semi-skimmed in-bottle sterilized milk, 153.8 g  
145 kg<sup>-1</sup> of water, 7.7 g kg<sup>-1</sup> of salt (NaCl) and 1.5 g kg<sup>-1</sup> of either  $\kappa$ -C or XG ([Alvarez et al.,  
146 2009](#)), using a TM 31 food processor (Vorwerk España, M.S.L., S.C., Madrid, Spain). The  
147 ingredients were first heated to 90 °C (17 °C min<sup>-1</sup>) and kept at 90 °C for 30 min (blade  
148 speed: 0.10 × g). Shearing was performed with a propeller. The amount of evaporated liquid  
149 was determined by weighing the ingredients before and after the first cooking and then  
150 replaced by adding milk. In terms of processibility, there were serious difficulties in cooking  
151 SPI together with the rest of the ingredients, especially when SPI levels were over 45 g kg<sup>-1</sup>.  
152 The SPI concentration of 15-60 g kg<sup>-1</sup> which had previously been hydrated at a ratio of SPI to  
153 water of 1:5 was then added at this point. **Water used to hydrate SPI was removed from initial  
154 water content (153.8 g kg<sup>-1</sup>).** Next, all the ingredients were cooked for an additional 5 min at

155 90 °C. The mash was ground for 40 s (blade speed: 80 × g) and 20 s (blade speed: 450 × g),  
156 and then homogenized immediately through a stainless steel sieve (diameter 1.5 mm). The  
157 average final pH of MPs without and with added SPI ranged between 5.9 and 6.0, and  
158 remained unmodified by a freeze/thaw cycle. Two batches were continuously being prepared  
159 and blended and half of each fresh blend (FM potatoes) was analysed immediately whilst the  
160 other half was frozen and thawed (F/TM potatoes). Each MP composition was prepared twice  
161 but in different weeks to assure the appropriate experiment randomization.

162

### 163 *2.3. Freezing, thawing and heating procedures*

164

165 Following their preparation, MP samples were placed on flat freezing and microwave  
166 thawing trays and then frozen by forced convection with liquid nitrogen vapour in an Instron  
167 programmable chamber (model 3119-05, -70/+250 °C) at -60 °C until their thermal centres  
168 reached -24 °C. After freezing, the samples were packed in polyethylene plastic bags, sealed  
169 under light vacuum (-0.05 MPa) on a Multivac packing machine (Sepp Haggemüller KG,  
170 Wolfertschwenden, Germany), and placed in a domestic freezer for storage at -24 °C. Packed  
171 frozen samples were then thawed in a Samsung M1712N microwave oven (Samsung  
172 Electronics S.A., Madrid, Spain) by heating for 20 min at an output power rating of 600 W.  
173 After thawing, the temperature reached at the product thermal centre was measured in all  
174 cases (+85 ± 3 °C). Samples were brought to 55 °C by placing them in a Hetofrig CB60VS  
175 water-bath (Heto Lab Equipment A/S, Birkerød, Denmark). The sample testing temperature  
176 was maintained at 55 °C as this is the preferred temperature for consumption of MPs ([Alvarez  
177 et al., 2011](#)).

178

### 179 *2.4. Rheological characterization. Oscillatory shear measurements*

180

181 A Bohlin CVR 50 controlled stress rheometer (Bohlin Instruments Ltd., Cirencester, UK)  
182 was used to conduct SAOS experiments using a plate-plate sensor system with a 2 mm gap  
183 (PP40, 40 mm) and a solvent trap to minimize moisture loss during tests. After loading the  
184 sample, there was a 5-minute waiting period to allow the sample to recover and reach 55 °C.  
185 Temperature control at 55 °C was achieved with a Peltier Plate system (-40 to +180 °C;  
186 Bohlin Instruments). In order to determine the linear viscoelastic (LVE) region, the first stress  
187 sweeps were run at a constant frequency ( $\omega$ ) of 1 rad s<sup>-1</sup> over a shear stress range of 3-300 Pa.  
188 The LVE range was limited to that amplitude range for which the complex modulus ( $G^*$ ) was  
189 constant (Navarro et al., 1997). Phase angle ( $\delta$ , °), storage modulus ( $G'$ , Pa) and loss modulus  
190 ( $G''$ , Pa) values were also registered within the LVE region. The  $G'$  represents the non-  
191 dissipative component of mechanical properties and is characteristic of elasticity, while  $G''$   
192 represents the dissipative component of the mechanical properties and is characteristic of  
193 viscous flow (Mohamed & Xu, 2003). In addition, a parameter was defined from the stress  
194 sweeps to characterize fluid behaviour for the nonlinear viscoelastic range ( $\alpha$ , fluid-like  
195 relative angle), namely the ratio between  $\delta$  measured at  $\gamma = 2 \times 10^{-1}$  to the phase angle  
196 corresponding to a pure fluid ( $\delta = 90^\circ$ ) (Navarro et al., 1997). Next three frequency sweeps  
197 were performed over the  $\omega$  range of 0.1-100 rad s<sup>-1</sup>, and again the  $\delta$ ,  $G'$  and  $G''$  values were  
198 registered at 1 rad s<sup>-1</sup>. Given that the appearance of the data on logarithmic data was nearly  
199 linear, a power law model (Eqs. 1 and 2) was used to characterize the frequency dependence  
200 of both moduli (Alvarez et al., 2011), from the following equations:

$$201 \quad G' = G_0' \cdot \omega^{n'}$$
(1)

$$202 \quad G'' = G_0'' \cdot \omega^{n''}$$
(2)

203 Where  $G_0'$  and  $G_0''$  are elastic and viscous moduli at 1 rad s<sup>-1</sup> respectively, and exponents  $n'$   
204 and  $n''$  denote the influence degree of  $\omega$  on both moduli.



205 Additionally, the structural differences between MP samples are quantifiable in terms of  
206 quality factor  $Q$  (Eq. 3) (angular frequency  $6.28 \text{ rad s}^{-1}$ ), a term frequently used in mechanical  
207 oscillatory systems. It is dimensionless quantity and represents the degree of damping of an  
208 oscillator (Campo-Deaño et al., 2010).

$$209 \quad Q = 2\pi(G_0' / G_0'') \omega^{(n'-n'')} \quad (3)$$

210 As a new sample was used each time for the dynamic tests, the resulting values were  
211 average values of the four determinations.

212

### 213 *2.5 Large deformation analyses*

214

215 Back extrusion (BE) and cone penetration (CP) mechanical tests were performed in order  
216 to study the empirical rheological behaviour of the semisolid-like samples. Both experiments  
217 were performed using a TA.HDPlus Texture Analyser (Stable Micro Systems Ltd,  
218 Godalming, UK) equipped with a 300 N load cell. During tests, MP samples were kept at 55  
219 °C by means of a Temperature Controlled Peltier Cabinet (XT/PC) coupled to a separate heat  
220 exchanger and a proportional-integral-derivative control unit. To perform BE tests, a rig  
221 (model A/BE, Stable Micro Systems) was used consisting of a flat 45 mm diameter perspex  
222 disc plunger that was driven down into a larger perspex cylinder sample holder (50 mm  
223 diameter) in order to force the MP samples to flow upwards through the concentric annular  
224 space between the plunger and the container. The measuring cup was filled with  $50 \pm 1 \text{ g}$  of  
225 MPs which were extruded to a distance of 20 mm at a  $2 \text{ mm s}^{-1}$  compression rate. At this  
226 point (most likely the maximum force), the probe returns to its original position. The area  
227 under the curve up to the “peak” or maximum force is taken as a measurement of BE  
228 consistency (N s), so that the higher the value the thicker the consistency of the sample. For  
229 performing the CP tests, a TTC (Texture Technologies Corporation) spreadability rig

230 (HDP/SR, Stable Micro Systems) was used, consisting of a 45 degree conical perspex probe  
231 (P/45 C) that penetrated a conical sample holder containing  $7 \pm 0.1$  g of MP product to a  
232 distance of 17.5 mm at a  $3 \text{ mm s}^{-1}$  compression rate. The CP work required per displaced  
233 volume ( $\text{J m}^{-3}$ ) to accomplish penetration was calculated from the area under the curve up to  
234 the “peak” or maximum penetration force. All measurements were repeated at least four  
235 times.

236

## 237 *2.6. Scanning electron microscopy (SEM)*

238

239 MP microstructure was examined by using a Hitachi S-2100 Scanning Electron  
240 Microscope (Hitachi, Ltd., Tokyo, Japan) (National Center for Metallurgical Research  
241 (CENIM)-CSIC). MP samples were air-dried, then mounted and sputter-coated with Au (200  
242 A approx.) in an SPI diode sputtering system metallizer. Micrographs were taken with a  
243 digital system Scanvision 1.2 of Röntgenanalysen-Technik (RONTEC) (GmbH, Berlin,  
244 Germany) (800x1.200 pixel).

245

## 246 *2.7. Statistical analysis*

247

248 A two-way ANOVA with interaction was applied to evaluate how SPI concentration and  
249 performance or not of a freeze/thaw cycle affected the rheological and instrumental textural  
250 properties. Minimum significant differences were calculated using Fisher’s least significant  
251 difference (LSD) tests with a 99% confidence interval. Analysis of variance and correlation  
252 was performed by using Statgraphics® software version 5.0 (STSC Inc., Rockville, MD,  
253 USA).

254

### 255 3. Results and discussion

256

#### 257 3.1. Effect of SPI concentration and freeze/thaw cycle on viscoelastic properties of MP

258

259 The common tests performed using small-amplitude oscillatory shear analyses are stress  
260 sweeps (for controlled stress rheometers), frequency sweeps, time sweeps, and temperature  
261 sweeps. Stress sweeps of FM potatoes at the different SPI concentrations (0-60 g kg<sup>-1</sup>) are  
262 shown in Fig. 1. Dynamic curves of storage modulus  $G'$  (elastic component) and loss  
263 modulus  $G''$  (viscous component) are presented as functions of strain  $\gamma$  over four decades of  
264 strain at a constant oscillation frequency of 1 rad s<sup>-1</sup>. Stress sweeps of F/TM potatoes were  
265 similar (curves are not shown). As an example, Fig. 1 also shows the complex modulus  $G^*$   
266 (measurement of the overall resistance (elastic and viscous)) of FM potatoes without added  
267 SPI. Similar behaviour was observed for the rest of the samples. This is an appropriate test for  
268 analyzing the gel character ( $G' > G''$ ) of samples, since as long as the strain amplitudes are  
269 below the limiting value ( $\gamma_{\max}$ ) the  $G^*$  pattern has a plateau value, indicating that the gel  
270 structure is stable under these conditions (Campo-Deaño et al., 2010). In all MP samples, both  
271  $G'$  and  $G^*$  moduli showed similar values at low deformations ( $< 0.003$ ), indicative of the low  
272 contribution of the viscous component  $G''$  to the viscoelastic properties of the systems.

273 The average value of the ratio  $G^*/G'$  calculated for the complete LVE domain ranged  
274 from 1.04 to 1.05 in FM potatoes and between 1.04 and 1.06 in F/TMs (Table 1). The highest  
275 ratio corresponded to the F/TM-SPI60 samples. Therefore, this result shows that the addition  
276 of SPIs at the highest concentration, increased the  $G''$  contribution to the viscoelastic  
277 properties of the F/TM potatoes in the LVE range. As freezing progresses and water migrates  
278 to form ice crystals, there is an increase in protein-protein interactions via hydrophobic and  
279 ionic forces resulting in further protein denaturation and protein aggregate formation (Xiong,

280 1997). It is apparent that a freeze/thaw cycle modulates SPI aggregation and gelation  
281 depending on SPI concentration and solvent properties (e.g., water activity,  $a_w$ ). It is well  
282 known that freezing reduces the  $a_w$  due to ice formation and the high concentrations of solutes  
283 in unfrozen water (Canet, 1989). A higher SPI content together with a reduced  $a_w$  made the  
284 water-SPI protein interaction less effective, promoting increased relative motion between  
285 domains of the superstructure, then the dissipated energy increases, thus explaining the more  
286 viscous-liquid behaviour observed in the F/TM-SPI60 samples.

287 The LVE range is limited by  $G'_{\max}$  and  $\gamma_{\max}$  (Fig. 1). The LVE domain determined for  
288 both FM and F/TM potatoes is shown in Table 1. SPI concentration had a significant effect on  
289 maximum strain, but the aspect most worthy of note is that mainly, when comparing the effect  
290 of a freeze/thaw cycle on a particular formulation, FM and F/TM samples differed in terms of  
291 fragility. At greater SPI concentrations (45 and 60 g kg<sup>-1</sup>),  $\gamma_{\max}$  was significantly lower in the  
292 FM samples than in their F/TM counterparts, indicating that F/TM-SPI45 and F/TM-SPI60  
293 samples can withstand higher strains without undergoing structural modifications. One factor  
294 accounting for the higher  $\gamma_{\max}$  values found in these frozen/thawed samples as compared to  
295 their fresh counterparts is that around coarser aggregates, stress amplification will occur (van  
296 Vliet, 1988). This may result in the strain being greater nearer the particle than in the linear  
297 region. A similar observation was reported by Zhu et al. (2008) for  $\kappa$ -C and soybean glycinin  
298 mixed gels and the authors concluded that both the glycinin and the  $\kappa$ -C formed a biphasic  
299 network.

300 Outside the LVE region, the viscous component gained in importance and  $G^*$  values were  
301 much greater than  $G'$  in all systems (Fig. 1). Above the LVE limit,  $G^*$  and  $G'$  decreased  
302 rapidly in all samples, indicating that the structure was highly prone to deformation. After  
303 structural breakdown, dynamic measurements quantified the liquid-like character of the MP  
304 samples characterized by the fluid-like relative angle  $\alpha$  as previously defined (Table 1). In

305 both FM and F/TM potatoes,  $\alpha$  values tended to decrease with increasing SPI concentrations  
306 up to 30 g kg<sup>-1</sup>. The lowest  $\alpha$  values corresponded to FM-SPI30 and F/TM-SPI30 samples. At  
307 SPI concentrations of more than 30 g kg<sup>-1</sup>, the  $\alpha$  values again increased. The highest  $\alpha$  values  
308 were also observed in both FM-SPI60 and F/TM-SPI60 samples, reflecting a more fluid-like  
309 behaviour with low viscosity after breakdown ( $\alpha \rightarrow 1$ ), characterized by a weak structure with  
310 poor recovery (Navarro et al., 1997). By adding 15 and 30 g kg<sup>-1</sup> SPI in the nonlinear range, it  
311 is possible that the two main coexisting structures (amylose/amylopectin matrix and SPI  
312 aggregates) supplemented each other and the protein properties added to those of the gel  
313 matrix present, as reflected by the lower  $\alpha$  values obtained for these samples (more solid-like  
314 than liquid characteristics).

315 Note that the FM-SPI45 and FM-SPI60 samples that showed a more significant rigid  
316 structure than their F/TM-SPI45 and F/TM-SPI60 counterparts in the LVE range (higher  
317  $G'_{\max}$  values), also had a less significant fluid-like character with superior viscosity after  
318 breakdown (Table 1). In contrast, although the FM-SPI30 sample presented a more significant  
319 rigid structure than its F/TM-SPI30 counterpart in the LVE range, it had more fluid-like  
320 characteristics than the F/TM samples after breakdown (a higher  $\alpha$  value). In turn, FM-SPI0  
321 and FM-SPI15 samples that showed a slightly less rigid structure than their F/TM-SPI0 and  
322 F/TM-SPI15 counterparts in the LVE range (lower  $G'$  values), also had a more fluid-like  
323 character with inferior viscosity after breakdown, even though in the lower SPI concentrations  
324 differences between the  $\alpha$  values of fresh and processed samples were non-significant. The  
325 addition of 30 g kg<sup>-1</sup> SPI produced a change in rheological behaviour, probably due to the  
326 thermodynamic incompatibility typical of a lot of protein-polysaccharide systems  
327 (Tolstoguzov, 1985). Thermodynamic incompatibility, on the other hand, involves the  
328 spontaneous separation into two solvent-rich phases, one composed predominantly of protein,  
329 and the other of polysaccharide. This is caused by demixing nondilute protein and

330 polysaccharide solutions under the influence of net repulsive protein-polysaccharide  
331 interactions (Liao et al., 1996; Zhu et al., 2008).

332 pH has also been mentioned as an important factor in the SPI gelation process (Nagano,  
333 Hirotsuka, Mori, Kohyama, & Nishinari, 1992; Tseng, Xiong, & Boatright, 2008; Turgeon &  
334 Beaulieu, 2001). SPI behaviour is closely related to the isoelectric point, which is in the  
335 region of 4.5 for SPI (Gennadios, Brandenburg, Weller, & Testin, 1993). As indicated above,  
336 the final pH of MP samples ranged from 5.9 to 6, and therefore the majority of SPI globulins  
337 would be negatively charged. Under these conditions, the electrostatic repulsive force  
338 between SPI proteins and negatively charged phosphate groups on anionic potato starch  
339 would become predominant, thereby preventing interaction between amylose/amylopectin  
340 matrix and protein molecules. In addition, this fact would facilitate the formation of two  
341 separated phases. Incompatible polymers, where the different polymers are repulsive and/or  
342 when the two types of polymers show varying degrees of affinity towards the solvent, form  
343 phase-separated gels (Turgeon & Beaulieu, 2001). Consequently, as the SPI concentration  
344 was increased further, phase separation occurred and  $\alpha$  values increased. These results may be  
345 useful for process engineering calculations and equipment design in the industrial production  
346 of SPI-enriched MP.

347 To better understand the structural changes that took place in the SPI-based MP structures,  
348 the influence of frequency in their viscoelastic properties was studied at 55 °C. Mechanical  
349 spectra provide essential information about gel structure and can be used to determine the  
350 behaviour of cross-linked proteins which are fixed by chemical bonds, forming a three-  
351 dimensional network (Campo-Deaño et al., 2010). Fig. 2 shows the evolution of  $G'$  and  $G''$  in  
352 the LVE range for F/TM potatoes with added SPI at 0-60 g kg<sup>-1</sup>. Similar mechanical spectra,  
353 without a qualitative change in the evolution of these functions, were obtained for FM  
354 counterparts at each concentration used. In all cases,  $G'$  was higher than  $G''$  for the complete

355  $\omega$  range studied, indicating elastic solid behaviour. In each food, the rheological behaviour is  
356 directly related to its formulation; the conformational changes experienced by potato starch  
357 were largely responsible for the predominantly elastic behaviour of the systems. In addition,  
358 double logarithmic plots of  $G'$  and  $G''$  vs. frequency resulted in straight lines with positive  
359 slopes of small magnitude ( $0.17 \leq n' \leq 0.20$  for  $G'$ , and  $0.08 \leq n'' \leq 0.15$  for  $G''$ ). Therefore,  
360 based on  $G'$  and  $G''$  frequency dependence values, SPI-based MP structures may be classified  
361 as weak gels.  $G''$  tends towards an equilibrium value in which the limited dependence of the  
362 frequency indicates the presence of a network arrangement (Alvarez et al., 2011). The higher  
363  $n'$  and  $n''$  values were obtained for F/TM-SPI60 samples indicating that these systems  
364 possessed networks which were transient in time and involved specific interactions between  
365 denser and less flexible particles, such as SPI aggregates. Mainly, when  $60 \text{ g kg}^{-1}$  SPI was  
366 added to the MP, the system clearly showed a less elastic behaviour, reflecting the  
367 development of a hindered potato starch three-dimensional internal structure (Fig. 2). The  
368 underlying phenomena that determine the observed reduction in rigidity would be  
369 dissociation, denaturation, and aggregation of SPI (Puppo et al., 2000; Sorgentini et al., 1995).

370 In turn, Table 2 shows the effects of SPI concentration and a freeze/thaw cycle on the  
371 values of the rheological properties derived from the oscillatory tests at  $1 \text{ rad s}^{-1}$ . The analysis  
372 of variance showed that SPI concentration had a significant effect ( $P < 0.01$ ) on the  $\delta$ ,  $G'$ ,  $G''$   
373 and  $Q$  values while a freeze/thaw cycle did not significantly affect the  $\delta$  and  $Q$  values of the  
374 samples. Furthermore, the binary interaction did not significantly affect the oscillatory  
375 rheological properties of the samples. This means that the effect of adding SPIs on oscillatory  
376 measurements in the LVE range is produced independently of whether or not the systems is  
377 subjected to a freeze/thaw cycle. Only the samples with added SPIs at  $60 \text{ g kg}^{-1}$  had a  
378 significantly higher  $\delta$  value than the samples without added SPI, again indicating that the  
379 highest concentrations of added SPIs produced a decrease in the final gel rigidity. Certainly,

380 no interaction between the amylose/amylopectin matrix and the dispersed SPI particles was  
381 established as reflected by a significant decrease in system viscoelasticity ( $G'$  and  $G''$  values)  
382 with increasing SPI concentration (Fig. 2). Likewise, no evidence was observed of any  
383 significant interaction between whey protein isolate and  $\kappa$ -C (Hemar et al., 2002).

384  $Q$  factor unifies parameters which provide structural information of different kinds:  $G_0'$   
385 and  $G_0''$  are related to the strength of the intermolecular interactions and  $n'$  and  $n''$  to the  
386 extent and stability of the network (Campo-Deaño et al., 2010). As it can be seen in Table 2,  
387 MP samples without added SPIs presented significantly higher  $Q$  values; there was a  
388 significant lowering of  $Q$  factor as SPI concentrations increased, confirming a disruptive  
389 effect of SPI aggregates on the amylose/amylopectin network. This behaviour is typical of  
390 gels filled with deformable particles (Jampen, Britt, Yada, & Tung, 2001). According to the  
391 latter authors, in gels containing deformable particles, the linear decrease in  $G'$  in line with  
392 increasing volume fractions is due to particle compliance under stress or to particle separation  
393 from the matrix, thereby causing gel weakening. The influence of particle-matrix interactions  
394 was also studied by van Vliet (1988) who found that a linear decrease in gel strength  
395 accompanied by an increase in volume fractions only occurred with non-interacting gel  
396 materials. This finding was attributed to the formation of aqueous boundary layers around  
397 each particle so that there was no adhesion between the particle and the matrix. The existence  
398 of an aqueous boundary layer may be a viable explanation for the data in the present study. especially at the higher SPI levels, because of the large amounts of water in these MP  
399 systems. As stress is applied to the system, small amounts of water may be released from the  
400 gelatinized starch gel, thus forming an aqueous boundary layer around the SPI aggregates.  
401 This layer would reduce any interactions with the gel matrix and lead to the formation of  
402 weak points in the gelatinized starch gel. Consequently, when these gels suffer small  
403 deformations, they behave as if filled with particles with the rheological properties of water.  
404



405 On the other hand, it is important to clarify that for studying protein gel formation, the  
406 common tests performed using small-amplitude oscillatory shear analyses are time sweeps  
407 (Nagano et al., 1992). Therefore protein dispersions are consecutively heated from 20 to 95  
408 °C, held at 95 °C for 30 min, cooled to 20 °C and then held at 20 °C for at least 15 min  
409 (Lakemond, de Jongh, Paques, van Vliet, Gruppen, & Voragen, 2003; Tseng et al., 2008).  
410 Generally, the gels undergo major structural development observed especially during the  
411 cooling phase, characterized by an increase in both the  $G'$  and  $G''$  values. It is well known  
412 that heating stabilizes hydrophobic bonds, and that hydrogen bonds are stabilized with  
413 decreasing temperature (Puppo et al., 2000). In this study, SPI was only heated in the  
414 presence of the other ingredients at 90 °C for 5 min, and then cooled to 55 °C (see subsection  
415 2.2). This brief heat treatment of SPI dissociated the compact glycinin and  $\beta$ -conglycinin  
416 oligomers into monomers and, in doing so, the hydrophobic groups were exposed (Tseng et  
417 al., 2008). However, no attempt was made to determine whether the structural changes  
418 detected in the MPs *via* rheological behaviour were sensitive to the time of heating or cooling  
419 times. It is expected that a lower cooling temperature and an extension of the cooling phase  
420 would result in a further strengthening of the protein structure. However, the thermal  
421 conditions for SPIs were in agreement with the standards for preparing this type of semisolid  
422 MP product (Alvarez et al., 2011).

423 Furthermore, both dynamic moduli were higher in the FM samples than in the F/TM ones  
424 (Table 2). It has been reported that freeze treatment increased the hydrophobicity of soy  
425 protein regardless of the heating treatment (Noh, Kang, Hong, & Yun, 2006). Because  
426 electrostatic interactions are one of the major forces maintaining protein tertiary and  
427 quaternary structures, an abrupt increase in ionic strength or salt concentration in the non-  
428 frozen phase can cause competition with existing electrostatic bonds, which in turn leads to  
429 extensive aggregation of the protein structure (Xiong, 1997). Hence, increased ionic strength

430 associated with freezing leads to the formation of coarser SPI aggregates. Furthermore, with  
431 respect to the F/TM samples in the present study, the microwave thawing treatment (a second  
432 heating) probably brought about a loss of solubility and changes in the soluble and insoluble  
433 fractions of SPIs. After thawing (heating up to 85 °C) additional denaturation and aggregation  
434 of the remaining SPI could be expected to occur.

435 Nevertheless, when the SPI network structure becomes coarser, the ability of the gels to  
436 retain water decreases (Lakemond et al., 2003). An increase in the intensity of protein self-  
437 association means that water becomes a poorer solvent for the protein but a better solvent for  
438 the polysaccharides. Water held within a protein structure is generally categorized into the  
439 following two groups: (a) water that is bound to the protein molecule and is not available as a  
440 solvent, and (b) trapped water within a protein matrix, which is regarded as retained water  
441 (Egbert, 2004). During freezing, the rate and extent of protein-protein interaction could affect  
442 the performance of proteins in immobilizing water and ultimately in decreasing the  
443 viscoelastic properties of the final product. Analogously, freezing produced an increase in the  
444 range of viscous behaviour observed in the mechanical spectrum of unheated whey protein  
445 concentrate suspensions, which was attributed to protein aggregation that occurred during  
446 freezing (Meza, Verdini, & Rubiolo, 2010). Unexpectedly, the freeze/thaw cycle effect was  
447 not significant for the quality factor  $Q$  (Table 2); this result shows that, on the whole, the  
448 rheological quality of SPI-MP samples was maintained after freezing and thawing processes.

449

### 450 *3.2. Effect of SPI concentration and freeze/thaw cycle on textural properties of MP*

451

452 Typical mechanical profiles taken during BE and CP tests are shown in Fig. 3. BE  
453 consistency decreased linearly with increasing SPI content in the FM potatoes, although there  
454 were non-significant differences between the curves shown for FM-SPI15 and FM-SPI30

455 samples (Fig. 3a). In turn, in the F/TM potatoes, the maximum penetration force, and  
456 therefore the CP work per displaced volume, also decreased linearly with increasing SPI  
457 concentrations (Fig. 3b). In  $\kappa$ -C and soybean glycinin mixed gels, hardness decreased  
458 significantly as native glycinin concentrations increased, but increased considerably as  
459 denatured glycinin increased (Zhu et al., 2008). In the case of the F/TM potatoes, the decrease  
460 in CP work per displaced volume with increasing SPI content is consistent with Fig. 2, which  
461 shows that  $G'$  also decreased in the processed samples as the SPI concentration increased  
462 from 15 to 60 g kg<sup>-1</sup>.

463 Table 2 also shows the effects of SPI concentrations and a freeze/thaw cycle on the  
464 instrumental textural property values derived from the large deformation tests. The analysis of  
465 variance showed that SPI concentrations and the freeze/thaw cycle had a significant effect on  
466 both textural properties measured, apart from which binary interaction also significantly  
467 affected the textural properties of the MP samples. From variations in the BE consistency  
468 values based on SPI concentrations for both FM and F/TM potatoes shown in Fig. 4a, one can  
469 observe that SPI content decreased BE consistency in both FM and F/TM samples, although  
470 there were non-significant differences between FM-SPI30 and FM-SPI45 and between F/TM-  
471 SPI0 and F/TM-SPI15 samples. In the case of FM products, samples with 60 g kg<sup>-1</sup> of added  
472 SPIs had the lowest BE consistency values, while samples with 30 and 45 g kg<sup>-1</sup> of added  
473 SPIs had the highest BE consistency values. In turn, when the amount of added SPs was  
474 increased, F/TM samples with 30-60 g kg<sup>-1</sup> of added SPIs had significantly lower BE  
475 consistency values than the SPI-free control. Note that although F/TM-SPI0 and F/TM-SPI15  
476 samples had significantly higher BE consistency values than their FM-SPI0 and FM-SPI15  
477 counterparts, there were non-significant differences between the BE consistency values for  
478 FM and F/TM potatoes with 30 and 45 g kg<sup>-1</sup> of added SPIs, while the F/TM-SPI60 sample  
479 had a significantly lower BE consistency value than its FM-SPI60 counterpart. At F/TM-

480 SPI15 samples, this hardening effect could reflect the effect of dehydration inherent in the  
481 process of freeze-denaturation, since water molecules hydrate the protein and act as a  
482 lubricant within the protein network. [Li et al. \(2007\)](#) reported that the amount of water  
483 covering the surface of a protein in a fully hydrated state was around  $0.3 \text{ g g}^{-1}$  protein while  
484 the water content of a dried protein product was usually less than  $0.1 \text{ g g}^{-1}$ . At higher SPI  
485 concentrations, probably the softening produced by the reduced ability of SPI gels to retain  
486 water was greater to this hardening effect.

487 When SPI levels increased, the CP work values evolved differently for each of the FM  
488 and F/TM potatoes ([Fig. 4b](#)). Whilst in FM potatoes, adding  $45 \text{ g kg}^{-1}$  SPIs increased the CP  
489 work value, the addition of  $15, 30$  and  $60 \text{ g kg}^{-1}$  SPIs did not influence CP work. In contrast,  
490 the addition of  $30\text{-}60 \text{ g kg}^{-1}$  significantly decreased this CP work value in the F/TM potatoes.  
491 F/TM-SPI0 and F/TM-SPI15 samples also had significantly higher CP work values than their  
492 FM-SPI0 and FM-SPI15 counterparts, while F/TM-SPI30, F/TM-SPI45 and F/TM-SPI60  
493 samples had significantly lower CP work values than their fresh counterparts. The results of a  
494 freeze/thaw cycle effect on textural measurements are in agreement with those obtained for  
495 the fluid-like relative angle  $\alpha$  estimated outside the LVE range ([Table 1](#)). This result confirms  
496 that  $30 \text{ g kg}^{-1}$  would also appear to be close to the phase separation threshold in SPI-MP  
497 samples indicating a change in the rheological behaviour between unfrozen samples as  
498 compared to their frozen counterparts. This minimal bulk concentration of SPIs when phase  
499 separation occurs depends on the excluded volume of macromolecules, although it was  
500 reported that it exceeds 4% for globular protein-polysaccharides mixtures ([Tolstoguzov,](#)  
501 [2003](#)).

502 The relationships between oscillatory rheological properties and instrumental texture  
503 parameters were determined by multiple correlations (data not shown). Although there was  
504 significant correlation between BE consistency and both dynamic  $G'$  and  $G''$  moduli ( $r=0.72$ ),

505 as well as between CP work and both viscoelastic properties ( $r=0.67$ ), these correlations were  
506 quite low showing that small and large deformation tests responded differently to the  
507 structure. Different trends in small and large deformation rheological tests were also found by  
508 [Ravindra, Genovese, Foegeding, and Rao \(2004\)](#). Data on the increase or decrease in gel  
509 moduli with increasing volume fractions of filler obtained under small deformation test  
510 conditions may not simply be extended to the increase or decrease in gel strength when  
511 subjected to large deformations, although if there is interaction between the matrix and the  
512 filler material some similarities may be observed ([van Vliet, 1988](#)). Interestingly, in this  
513 study, when considering the F/TM samples separately, quite high correlations between  
514 viscoelastic properties and large deformation measurements ( $r\geq 0.94$ ) were established.

515

### 516 *3.3. Microstructure examination*

517

518 To achieve a better understanding of the rheological results and the effect of SPI  
519 concentrations and freezing, the microstructure of the systems was studied by SEM.  
520 Microphotographs of FM and F/TM potatoes without and with added SPIs at the intermediate  
521 ( $30 \text{ g kg}^{-1}$ ) and highest SPI concentrations used are shown in [Fig. 5](#). Cracks and differences in  
522 colour should be disregarded as they are not features of the different samples but a problem of  
523 sample preparation and image generation respectively. As shown by the rheological results,  
524 the effect of SPI on the microstructure depended on either SPI concentration or on whether  
525 the systems was subjected to a freeze/thaw cycle or not.

526 Both FM and F/TM samples without added SPIs ([Figs. 5a, d](#)) consist mainly of a  
527 continuous phase (amylose/amylopectin matrix) due to the disruption and complete  
528 solubilisation of the potato starch granules by heating. Micrographs revealed the presence of  
529 cell wall cementing materials as well as cell fragments are embedded in the continuous

530 solubilized starch matrix. In all the FM products, the shape of the potato cells could still be  
531 observed (Figs. 5a-c). In both SPI concentrations (Figs. 5b, c, e, f), a protein network structure  
532 can be seen composed of protein aggregate clumps and small SPI clusters, which are clearly  
533 distinguishable from the starch matrix. In the case of globular proteins two different types of  
534 gel network can be observed: fine-stranded and coarse networks (Lakemond et al., 2003).  
535 There are three major influences that determine the nature of the protein gel formed: (1)  
536 environmental conditions, such as pH, ionic strength, and mineral content; (2) protein  
537 composition, extent of denaturation, and concentration; and (3) processing conditions, such as  
538 heating and cooling rates (Turgeon & Beaulieu, 2001). The addition of cations (Mohamed and  
539 Xu, 2003) or pH values near the isoelectric point (over pH 4-6) results in less electrostatic  
540 repulsion between protein components thereby allowing aggregation prior to gel formation.  
541 The MP samples studied here contain either  $\text{Na}^+$ , from salt incorporation, or  $\text{Ca}^{2+}$  ions,  
542 proceeding mainly from added milk. The presence of both cations in the systems may  
543 possibly have led to an enhanced hydrophobic association of soy proteins, favouring the  
544 formation of these opaque gels defined as white aggregate or particulate gels. Tseng et al.  
545 (2008) also observed that SPI gels exhibited a particulate porous network structure.

546 In the F/TM samples (Figs. 5d-f), the tissue presents a more dehydrated appearance, since  
547 part of the intracellular water was drawn out osmotically when the product was thawed, due to  
548 a freezing-induced concentration of the cell mass and reduced water activity (Canet, 1989).  
549 Notably, most of the cells lost their spherical shape and were visibly shrunken, a fact which  
550 was also reflected in decreased rheological properties. Micrographs confirm that there was no  
551 thermal interaction between potato starch and SPIs, and two phases can be appreciated.  
552 Mixtures of  $\kappa$ -C with skimmed milk powder, milk protein concentrate, and sodium caseinate  
553 also showed phase separation (Hemar et al., 2002). Thermodynamic incompatibility  
554 (electrostatic repulsion and water partition between molecules) promoted association between

555 macromolecules of the same type, i.e. facilitated self-association of biopolymers  
556 (Tolstoguzov, 1985).

557 On the other hand, an increase in the intensity of protein self-association (the quantity of  
558 SPI clusters was higher) was observed by increasing SPI concentration or after a freeze/thaw  
559 cycle (Figs. 5c, f). The freeze/thaw cycle mainly enhanced the aggregation tendency of  
560 unfolded protein molecules thus increasing the particulate network. Apart from the foregoing,  
561 a pH value of 5.9/6 in combination with a high SPI concentration could have enhanced  
562 protein aggregation through attractive electrostatic interaction between the different SPI  
563 components (Nagano et al., 1992), producing sizeable and loosely associated clusters of  
564 aggregates. Samples with added 60 g kg<sup>-1</sup> SPI, which had the largest aggregates in SEM, also  
565 had the lowest  $G'$  values. It was also suggested that the bigger particles disrupted the matrix  
566 because they did not “fit” into the void spaces of the matrix (Jampen et al., 2001). Particle  
567 size differences may therefore partly account for the MPs rigidity minima obtained with  
568 higher SPI concentrations. The force applied to the system would be expected to result in  
569 deformation or energy absorption in both the amylose/amylopectin matrix and the SPI  
570 aggregate itself, leading to an overall structure characterized by lower rigidity.

571

#### 572 **4. Conclusion**

573

574 As the stimulus in texture perception is predominantly mechanical in nature, small and  
575 large deformation rheological measurements have been used to arrive at a mechanistic  
576 understanding of SPI-based MP systems. Both FM and F/TM potatoes with added SPIs can be  
577 considered as macromolecular gels containing dispersed SPI aggregates (fillers), which  
578 behave as deformable particles. This transition from a completely continuous phase  
579 (amylose/amylopectin matrix) to a system where the SPI aggregates are dispersed is shown by

580 a decrease in system viscoelasticity ( $G'$  and  $G''$  values) and large deformation measurements.  
581 Consequently, there is no interaction between the potato gel matrix and the dispersed SPI  
582 particles. The principal cause would appear to be the electrostatic repulsive force between the  
583 negatively charged SPI globulins and the anionic potato starch. The structures of the systems  
584 were even weakened to a greater extent by the freeze/thaw cycle, mainly because the gel  
585 properties (elasticity and viscosity) of the amylose/amylopectin matrix were reduced by  
586 coarsening of the SPI network structure associated with a decreased ability to retain water. 30  
587  $\text{g kg}^{-1}$  SPI would appear to be close to the phase separation threshold in SPI-MP samples,  
588 revealing a change in rheological behaviour due to thermodynamic incompatibility between  
589 solubilized potato starch and SPI. Despite the results obtained, matching the rheological  
590 behaviour of SPI-based MPs does not guarantee a corresponding matching of the sensory-  
591 perceived texture. A thorough knowledge of the sensory properties of the systems is  
592 subsequently needed. It is expected that, by adopting the texture-modifying properties of SPI,  
593 functional MPs can be prepared.

594



595 **Acknowledgements**

596       The authors wish to thank the Spanish Ministry of Science and Innovation for its financial  
597 support (AGL2007-62851), as well as P. Adeva, I. Amurrio and A. García of the Electron  
598 Microscopy Laboratory (CENIM-CSIC).

599

600 **References**

601

602 Alvarez, M. D., Fernández, C., Solas, M. T., & Canet, W. (2011). Viscoelasticity and  
603 microstructure of inulin-enriched mashed potatoes: influence of freezing and  
604 cryoprotectants. *Journal of Food Engineering*, 102, 66-76.

605 Campo-Deaño, L., Tovar, C. A., & Borderías, J. (2010). Effect of several cryoprotectants on  
606 the physicochemical and rheological properties of suwari gels from frozen squid surimi  
607 made by two methods. *Journal of Food Engineering*, 97, 457-464.

608 Canet, W. (1989). Quality and stability of frozen vegetables. In S. Thorne (Ed.),  
609 *Developments in Food Preservation* (pp. 1-50). London: Elsevier.

610 Egbert, W. R. (2004). Isolated soy protein: technology, properties and applications. In K. Liu  
611 (Ed.), *Soybeans as Functional Foods and Ingredients* (pp. 135-162). USA: AOCS  
612 Publishing.

613 Federal Register. (1998). Food labeling: health claim soy protein and coronary heart disease.  
614 *Federal Register*, 63, 62977–63015.

615 Gennadios, A., Brandenburg, A. H., Séller, C. L., & Testin, R. F. (1993). Effect of pH on  
616 properties of wheat gluten and soy protein isolate films. *Journal of Agricultural and*  
617 *Food Chemistry*, 41, 1835-1839.

618 Hashizume, K., Kakiuchi, K., Koyama, E., & Watanabe, T. (1971). Denaturation of soy  
619 protein by freezing. *Agricultural & Biological Chemistry*, 35, 449-459.

620 Hemar, Y., Hall, C. E., Munro, P. A., & Singh, H. (2002). Small and large deformation  
621 rheology and microstructure of  $\kappa$ -carrageenan gels containing commercial milk protein  
622 products. *International Dairy Journal*, 12, 371-381.

623 Jampen, S., Britt, I. J., Yada, S., & Tung, M. A. (2001). Rheological properties of gellan gels  
624 containing filler particles. *Journal of Food Science*, 66, 289–293.

625 Lakemond, C. M. M., de Jongh, H. H. J., Paques, M., van Vliet, T., Gruppen H., & Voragen,  
626 G. J. (2003). Gelation of soy glycinin; influence of pH and ionic strength on network  
627 structure in relation to protein conformation. *Food Hydrocolloids*, *17*, 365-377.

628 Li, X., Li, Y., Hua, Y., Qiu, A., Yang, C., & Cui S. (2007). Effect of concentration, ionic  
629 strength and freeze-drying on the heat-induced aggregation of soy proteins. *Food*  
630 *Chemistry*, *104*, 1410-1417.

631 Liao, H.-J., Okechukwu, P. E., Damodaran, S., & Rao, M. A. (1996). Rheological and  
632 calorimetric properties of heated corn starch-soybean protein isolate dispersions.  
633 *Journal of Texture Studies*, *27*, 403-418.

634 Meza, B. E., Verdini, R. A., & Rubiolo, A. C. (2010). Effect of freezing on the viscoelastic  
635 behaviour of whey protein concentrate suspensions. *Food Hydrocolloids*, *24*, 414-423.

636 Mohamed, A., & Xu, J. (2003). Effect of ionic strength and pH on the thermal and rheological  
637 properties of soy protein-amylopectin blend. *Food Chemistry*, *83*, 227-236.

638 Navarro, A. S., Martino, M. N., & Zaritzky, N. E. (1997). Correlation between transient  
639 rotational viscometry and a dynamic oscillatory test for viscoelastic starch based  
640 systems. *Journal of Texture Studies*, *28*, 365-385.

641 Nagano, T., Hirotsuka, M., Mori, H., Kohyama, K., & Nishinari, K. (1992). Dynamic  
642 viscoelastic study on the gelation of 7S globulin from soybeans. *Journal of Agricultural*  
643 *and Food Chemistry*, *40*, 941-944.

644 Noh, E. J., Kang, C., Hong, S. T., & Yun, S. E. (2006). Freezing of soybeans influences the  
645 hydrophobicity of soy protein. *Food Chemistry*, *97*, 212-216.

646 Puppo, M. C., Sorgentini, D. A., & Añón, M. C. (2000). Rheological study of dispersions  
647 prepared with modified soybean protein isolates. *Journal of the American Oil Chemists'*  
648 *Society*, *77*, 63-71.

649 Ravindra, P., Genovese, D. B., Foegeding, E. A., & Rao, M. A. (2004). Rheology of heated  
650 mixed protein isolate/cross-linked waxy maize starch dispersions. *Food Hydrocolloids*,  
651 *18*, 775–781.

652 Sorgentini, D. A., Wagner, JR., & Añón, M. C. (1995). Effects of thermal-treatment of soy  
653 protein isolate on the characteristics and structure-function relationship of soluble and  
654 insoluble fractions. *Journal of Agricultural and Food Chemistry*, *43*, 2471-2479.

655 Soya – Information about Soy and Soya Products. [http://www.soya.be/soy-protein-health-](http://www.soya.be/soy-protein-health-claim.php)  
656 [claim.php](http://www.soya.be/soy-protein-health-claim.php)

657 Tattiyakul, J., & Rao, M. A. (2000). Rheological behavior of cross-linked waxy maize starch  
658 dispersions during and after heating. *Carbohydrate Polymers*, *43*, 215-222.

659 Tolstoguzov, V. B. (1985). Functional properties of protein-polysaccharide mixtures. In J. R.  
660 Mitchell & D. A. Ledward (Eds), *Functional Properties of Food Macromolecules* (pp.  
661 171-202). New York: Elsevier Science.

662 Tolstoguzov, V. (2003). Thermodynamic considerations of starch functionality in foods.  
663 *Carbohydrate Polymers*, *51*, 99-111.

664 Tseng, Y.-C., Xiong, Y. L., & Boatright, W. L. (2008). Effects of inulin/oligofructose on the  
665 thermal stability and acid-induced gelation of soy proteins. *Journal of Food Science*, *73*,  
666 E44-E50.

667 Turgeon, S. L., & Beaulieu, M. (2001). Improvement and modification of whey protein gel  
668 texture using polysaccharides. *Food Hydrocolloids*, *15*, 583–591.

669 Utsumi, S., & Kinsella, J. E. (1985). Structure-function relationships in food proteins: subunit  
670 interactions in heat-induced gelation of 7S, 11S and soy isolate proteins. *Journal of*  
671 *Agricultural and Food Chemistry*, *33*, 297-303.

672 van Vliet, T. (1988). Rheological properties of filled gels: Influence of filler matrix  
673 interaction. *Colloid and Polymer Science*, *266*, 518-524.

674 Xiong, Y. L. (1997). Protein denaturation and functionality losses. In M. C. Erickson, & Y.-C.  
675 Hung (Eds.), *Quality in Frozen Foods* (pp. 111-140). New York: Chapman & Hall.  
676 Zhu, J. H., Yang, X. Q., Ahmad, I., Li, L., Wang, X. Y., & Liu, C. (2008). Rheological  
677 properties of  $\kappa$ -carrageenan and soybean glycinin mixed gels. *Food Research*  
678 *International*, *41*, 219-228.  
679

## Figure captions

680

681

682 **Fig. 1.** Typical dynamic curves showing the changes in storage modulus ( $G'$ , Pa) and loss  
683 modulus ( $G''$ , Pa) with strain (frequency  $1 \text{ rad s}^{-1}$ ) for fresh mashed potatoes (FM) with added  
684 SPI at 0, 15, 30 45 and  $60 \text{ g kg}^{-1}$ .

685 **Fig. 2.** Dynamic properties, storage modulus ( $G'$ , Pa) and loss modulus ( $G''$ , Pa) versus  
686 frequency ( $\text{rad s}^{-1}$ ) for frozen/thawed mashed potatoes (F/TM) with added SPI at 0, 15, 30 45  
687 and  $60 \text{ g kg}^{-1}$ .

688 **Fig. 3.** Typical force versus time curves generated by large deformation tests for mashed  
689 potato samples with added SPI at 0, 15, 30 45 and  $60 \text{ g kg}^{-1}$ . (a) Back extrusion (BE) curves  
690 of fresh mashed potatoes (FM). (b) Cone penetration (CP) curves of frozen/thawed mashed  
691 potatoes (F/TM).

692 **Fig. 4.** Large deformation measurements of both fresh (FM) and processed mashed potatoes  
693 (F/TM) with added SPI at 0, 15, 30, 45 and  $60 \text{ g kg}^{-1}$ . (a) Back extrusion (BE) consistency. (b)  
694 Cone penetration (CP) work per displaced volume.

695 **Fig. 5.** Microphotographs of mashed potato samples. (a) Fresh mashed potatoes without  
696 added SPI. (b) Fresh mashed potatoes with  $30 \text{ g kg}^{-1}$  added SPI (FM-SPI30). (c) Fresh  
697 mashed potatoes with  $60 \text{ g kg}^{-1}$  added SPI (FM-SPI60). (d) Frozen/thawed mashed potatoes  
698 without added SPI. (e) Frozen/thawed mashed potatoes with  $30 \text{ g kg}^{-1}$  added SPI (F/TM-  
699 SPI30). (f) Frozen/thawed mashed potatoes with  $60 \text{ g kg}^{-1}$  added SPI (F/TM-SPI60).

**Table 1**

Dynamic measurements for linear and nonlinear viscoelastic ranges of fresh (FM) and frozen/thawed (F/TM) mashed potatoes with added SPI at different concentrations.

System notation	$G^*_{\max}$ (Pa)	$G'_{\max}$ (Pa)	$\gamma_{\max}$ (°)	$G^*/G'^a$	$\alpha$
FM-SPI0	5273 ± 56 a	5019 ± 45 a	1.94 10 <sup>-3</sup> ± 9.01 10 <sup>-5</sup> d	1.04 ± 0.005 a	0.194 ± 0.003 b, c
F/TM-SPI0	5278 ± 82 a	5063 ± 47 a	1.25 10 <sup>-3</sup> ± 7.11 10 <sup>-5</sup> g	1.04 ± 0.002 a	0.189 ± 0.001 c, d
FM-SPI15	4211 ± 105 b	3980 ± 70 b	0.96 10 <sup>-3</sup> ± 9.87 10 <sup>-5</sup> a	1.05 ± 0.003 b	0.190 ± 0.002 c, d
F/TM-SPI15	4309 ± 95 b	4110 ± 97 b	0.94 10 <sup>-3</sup> ± 1.22 10 <sup>-5</sup> b	1.04 ± 0.002 a	0.189 ± 0.001 c, d
FM-SPI30	3617 ± 67 c	3477 ± 17 c	1.80 10 <sup>-3</sup> ± 8.31 10 <sup>-5</sup> d	1.04 ± 0.005 a	0.172 ± 0.004 e
F/TM-SPI30	3228 ± 18 d	3068 ± 81 d	1.45 10 <sup>-3</sup> ± 1.79 10 <sup>-5</sup> f	1.05 ± 0.001 b	0.161 ± 0.001 f
FM-SPI45	3104 ± 74 d	2983 ± 71 d	1.13 10 <sup>-3</sup> ± 4.11 10 <sup>-5</sup> g	1.04 ± 0.003 a	0.177 ± 0.002 e
F/TM-SPI45	2488 ± 71 e	2378 ± 32 e	1.63 10 <sup>-3</sup> ± 7.85 10 <sup>-5</sup> e	1.05 ± 0.001 b	0.186 ± 0.000 d
FM-SPI60	1867 ± 75 f	1775 ± 105 f	1.88 10 <sup>-3</sup> ± 3.01 10 <sup>-5</sup> d	1.05 ± 0.004 b	0.197 ± 0.004 b
F/TM-SPI60	1074 ± 103 g	1012 ± 117 g	3.23 10 <sup>-3</sup> ± 6.10 10 <sup>-5</sup> c	1.06 ± 0.002 c	0.210 ± 0.001 a
<i>LSD (99%)</i>	<i>176.08</i>	<i>168.31</i>	<i>1.15 10<sup>-3</sup></i>	<i>0.007</i>	<i>0.005</i>

<sup>a</sup>Ratio values correspond to the average value at the linear viscoelastic range. Different lower case letters in the same rheological property column and treatment type indicate significant differences ( $P < 0.01$ ).

**Table 2**

Effects of SPI concentration and a freeze/thaw cycle on oscillatory properties and quality factor  $Q$  and large deformation measurements of MP samples.

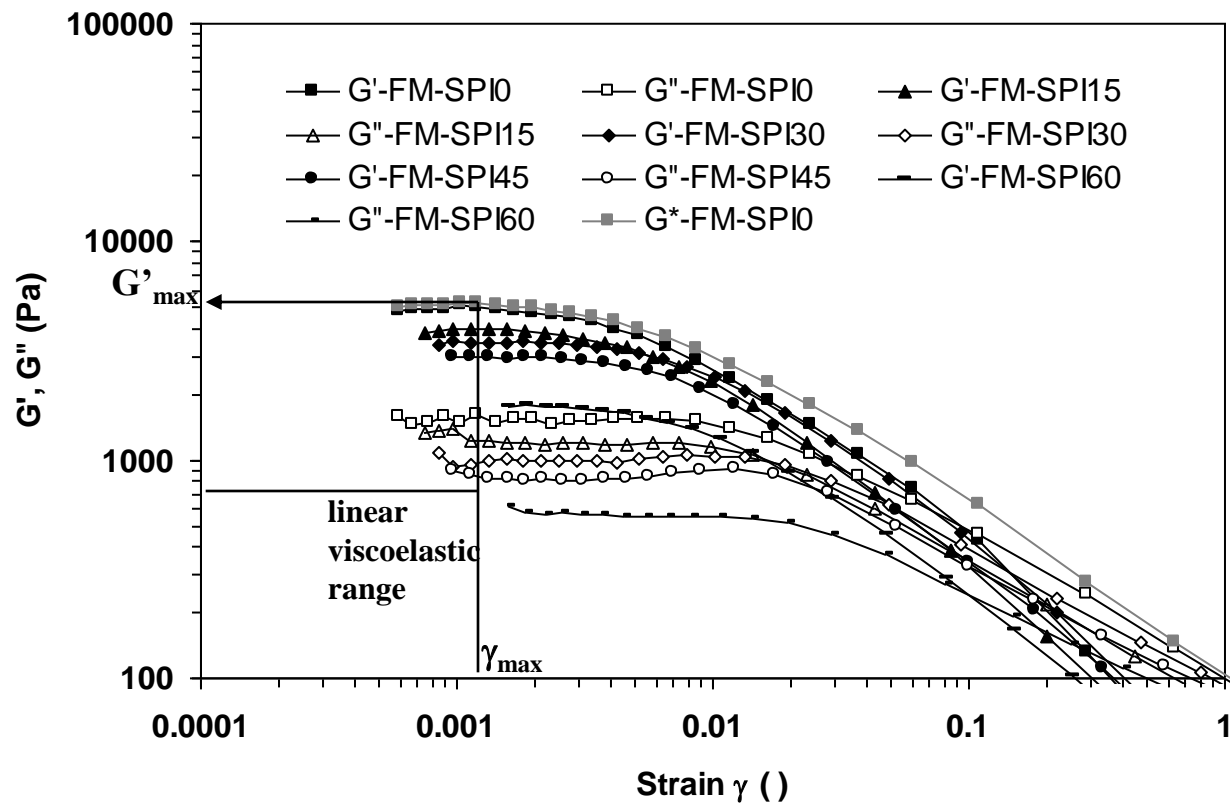
Source	$\delta$ (°)	$G'$ (Pa)	$G''$ (Pa)	$Q$	BE consistency (N s)	CP work per displaced volume (J m <sup>-3</sup> )
<b>Main effects:</b>						
A: SPI concentration (g kg <sup>-1</sup> )						
0	15.74 a	5314.00 a	1502.12 a	8.56 a	57.58 a	3630.66 a
15	16.00 a	4265.75 b	1221.00 b	8.20 b	52.63 b	3723.72 a
30	15.90 a	3247.00 c	911.45 c	8.13 b, c	48.13 c	3236.96 b
45	15.36 a	2881.87 d	815.60 c	7.91 c, d	50.27 c	3109.18 b
60	17.97 b	1553.25 e	498.66 d	7.70 d	37.31 d	2726.60 c
<i>P</i> values	<0.001	<0.001	<0.001	<0.001	<0.001	<0.001
<i>LSD</i> (99%)	1.49	343.50	131.23	0.29	1.81	186.54
B: Freeze/thaw cycle						
FM potatoes	15.76 a	3711.25 a	1048.66 a	8.06 a	46.71 a	3477.69 a
F/TM potatoes	16.62 a	3193.50 b	930.87 b	8.13 a	51.67 b	3093.16 b
<i>P</i> values	0.017	<0.001	<0.001	0.450	<0.001	<0.001
<i>LSD</i> (99%)	0.94	217.25	83.00	0.14	1.15	117.98
Interaction						
AB						
<i>P</i> values	0.484	0.053	0.208	0.899	<0.001	<0.001

Different lower case letters in the same column and factor studied indicate significant differences ( $P < 0.01$ ).



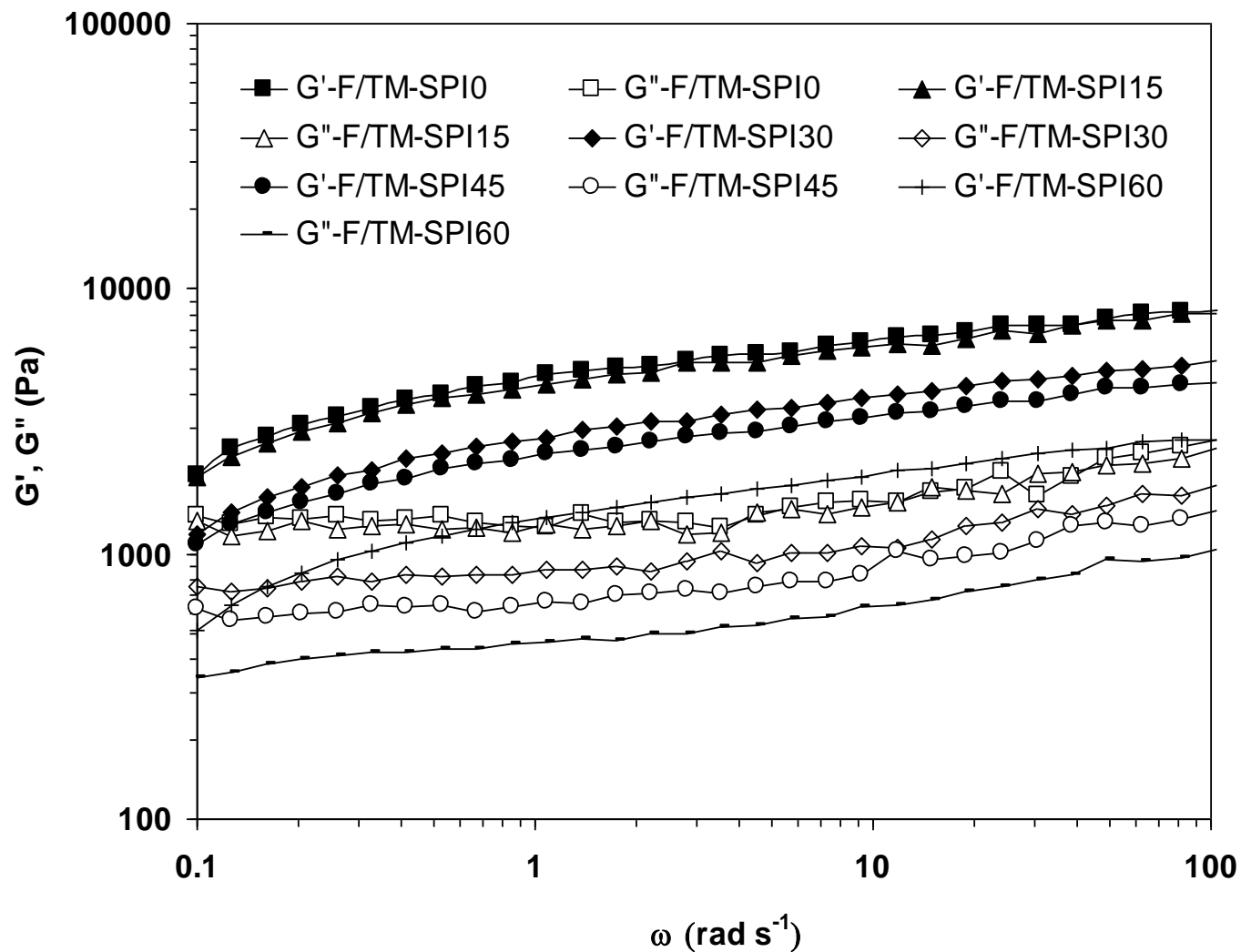
**Fig. 1.**

María Dolores Alvarez, Cristina Fernández, María Dolores Olivares, Wenceslao Canet



**Fig. 2.**

María Dolores Alvarez, Cristina Fernández, María Dolores Olivares, Wenceslao Canet



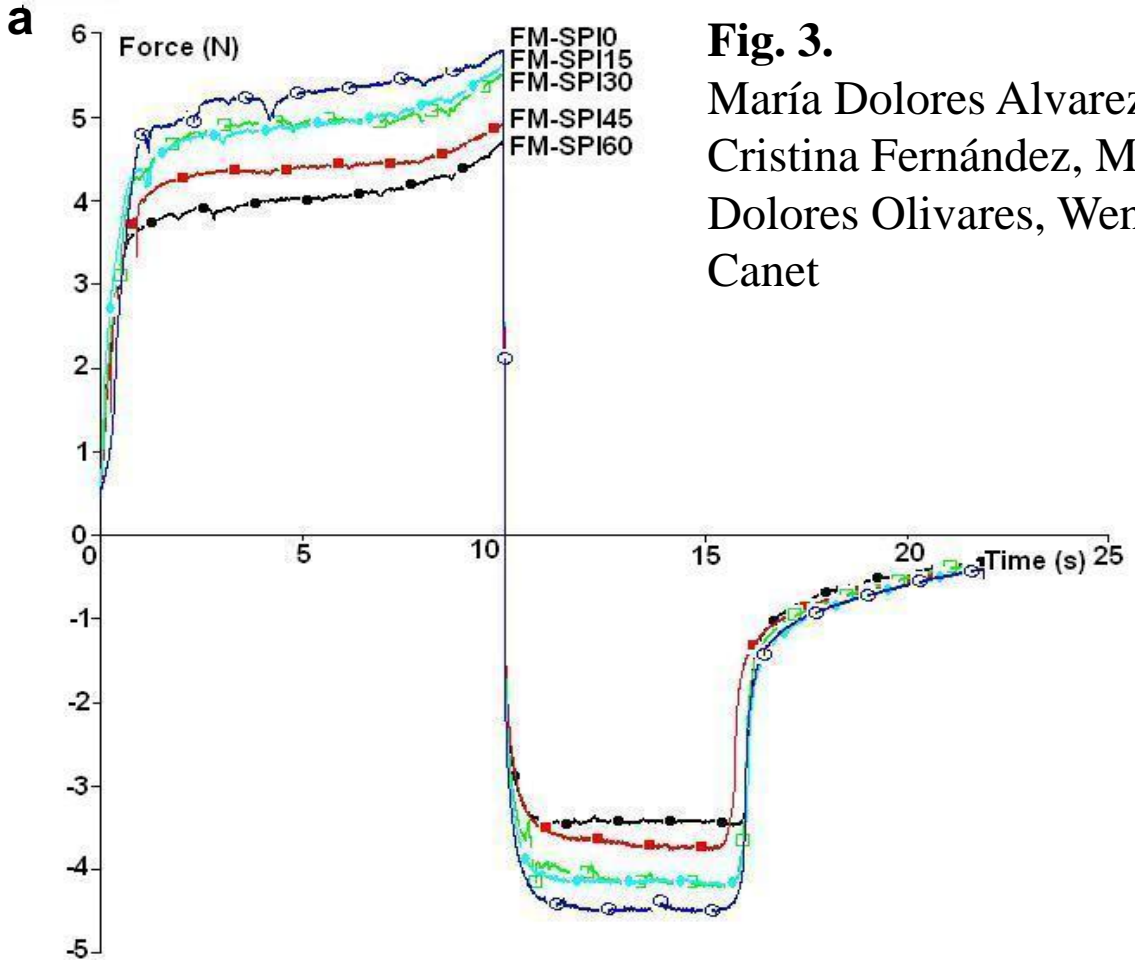


**Fig. 3.**

María Dolores Alvarez,  
Cristina Fernández, María  
Dolores Olivares, Wenceslao  
Canet

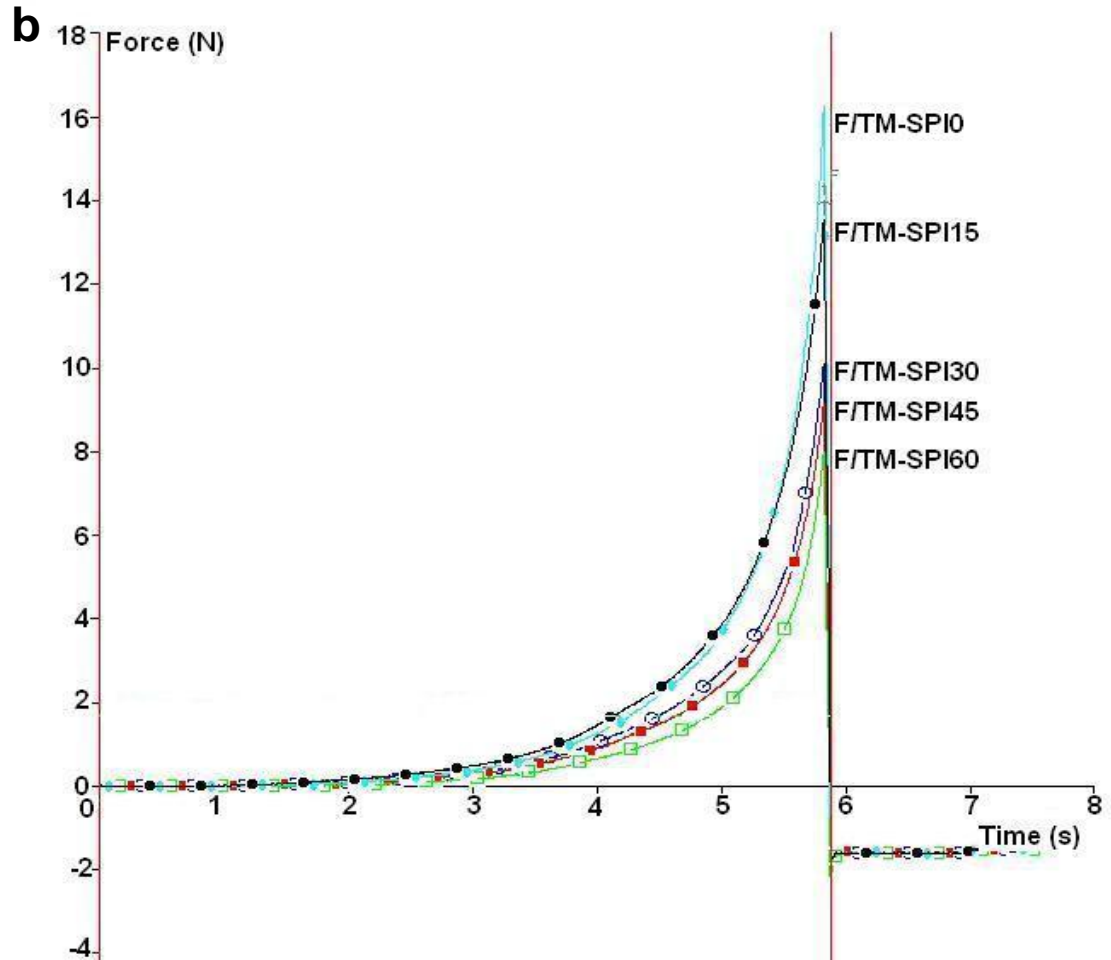


**Fig. 4.**

María Dolores Alvarez, Cristina Fernández, María Dolores Olivares, Wenceslao Canet

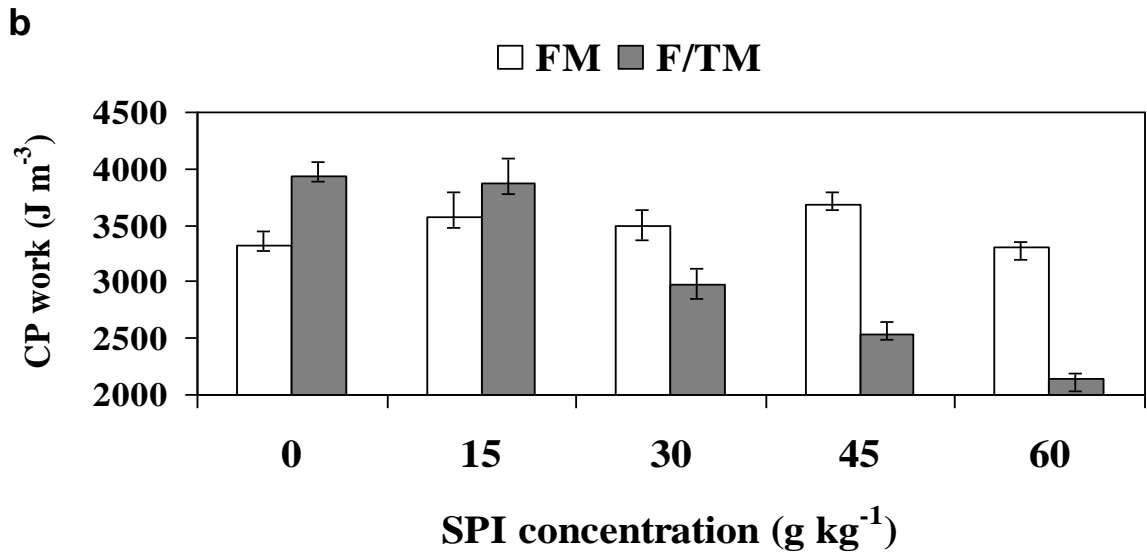
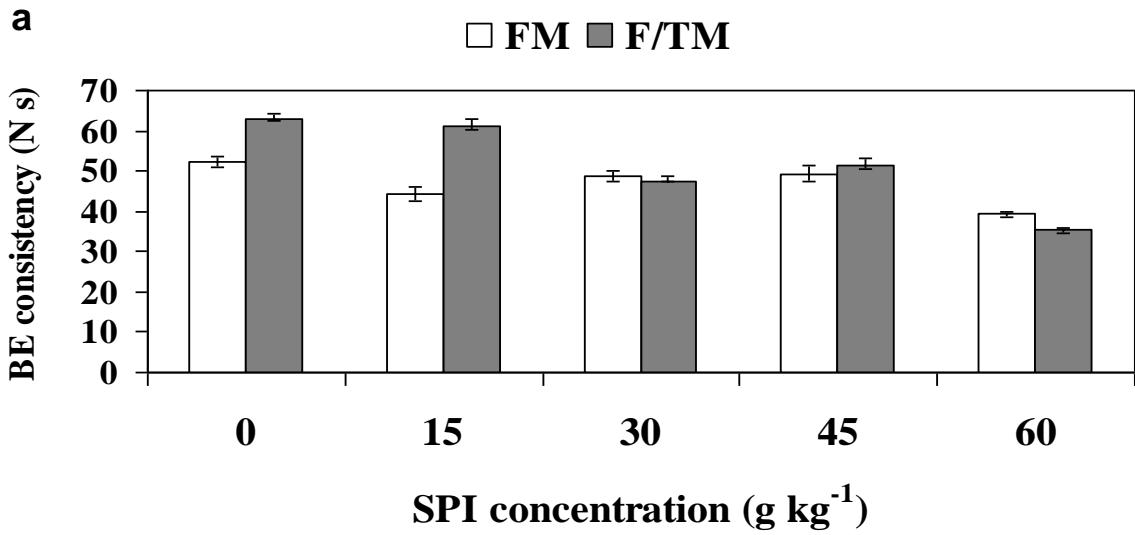


**Fig. 5.**  
María Dolores Alvarez, Cristina Fernández, María Dolores Olivares, Wenceslao Canet

